

# Synchronous Boost Converter Design for an E-Scooter Application and Comparison with Conventional Boost Converter

Mustafa Burak AKBAŞ<sup>1</sup>, Güven ONUR<sup>2</sup>, and Derya Ahmet KOCABAŞ<sup>3</sup>

<sup>1</sup>Istanbul Technical University, Istanbul, Türkiye  
mburakakbas@aselsan.com.tr

## Abstract

This study presents the performance of a designed Synchronous Boost Converter for an E-Scooter application and compares it with a Conventional Boost Converter. The study's primary objective is to boost the 12 Volt battery output to 24 Volts in a controllable manner and transmit this boosted voltage to the motor driver. This approach offers several advantages, including enhancing the stability of the input voltage, strengthening short-circuit resilience by increasing impedance on the motor side, reducing voltage ripple, and increasing the overload capacity of the motor by increasing 24 Volts when necessary. Simulations conducted in PLECS and control parameters obtained through the Bode Diagram Method were used to compare the performance of the Synchronous Boost Converter and Conventional Boost Converter. The study results indicate that the losses of the Synchronous Boost Converter have decreased by 45% compared to the Conventional Boost Converter, and its efficiency has reached 96.08%.

## 1. Introduction

As a result of the continuously increasing world population, the demand for electrical energy has also risen. Electricity is now utilized in almost every aspect of our lives, including industrial applications, motors, electric vehicles, household appliances, space applications, lighting, and electronic devices. At present, electricity is generated in power plants and renewable energy sources, and it is distributed to consumers through transmission networks. Ideally, grid voltage is sinusoidal, and maintaining the waveform stability is preferred. Despite having a single type of grid waveform, the required waveform and amplitude differ for each load. Additionally, a single load may require different waveforms and amplitudes at different times. This variability underscores the indispensable role of power electronics and their constituent components.

Power electronic components possess the capacity to **transmute** the form of voltage (alternating current/direct current, direct current/alternating current) and additionally **modulate** the amplitude and frequency within the identical electrical domain (alternating current/alternating current, direct current/direct current). **Fundamental applications encompass the amplification or attenuation of voltage levels** and the transformation of alternating current to direct current or conversely. These power electronic components further **facilitate system control**, thereby enabling dynamic adaptability to meet the requisites of the application and, through embedded software algorithms, **attain autonomous regulatory functionality**.

Among these power electronic components, the most **pivotal** and **ubiquitous** are DC-DC converters. The primary **archetypes** of DC-DC converters consist of buck, boost, buck-boost, Cuk, and flyback converters. These converters serve the **imperative function** of transmitting voltage from a power source to the voltage **stipulated** by the application. To **facilitate** this voltage **transformation**, these circuits necessitate electrical components such as inductors, capacitors, transformers, diodes, and semiconductor devices [1].

Boost converters, **specifically**, are **instrumental** in accommodating the elevated voltage requisites of diverse applications. They are **encompassed by a broader category that includes** buck converters, boost converters, buck-boost converters, Cuk converters, and flyback converters. To **accomplish this voltage augmentation**, these circuits **utilize** electrical components such as coils, capacitors, transformers, diodes, and semiconductor devices. Boost converters **elevate** the voltage from the power source to a **superior voltage level**, transferring it to the load. In numerous applications, the voltage from the source is **deficient for the operational requirements of the load**, necessitating an **escalation** in voltage. Consequently, boost converters are **extensively employed** across multiple industries. They find **utilization** in photovoltaic cells, battery power systems, energy storage systems, motor drive systems, and a **multitude of other applications** [2, 3, 4].

However, like other converters, boost converters also experience power losses, which reduce efficiency. The reasons for power losses in converter circuits can be categorized as conduction losses and component losses. In boost converters, a significant portion of these component losses results from the resistance present in the topology of the converter. In addition to the inherent power losses in systems, experiencing power losses in power electronic components such as converters is undesirable. Therefore, in modern times, instead of using diode elements in boost converters, semiconductor elements (MOSFET, IGBT, etc.) have begun to be used [5, 6, 7]. In this converter, there is already one semiconductor in use, and with the addition of a second semiconductor, replacing the diode, the total number of semiconductor elements becomes two. Due to the circuit topology, these semiconductor elements must operate synchronously. Hence, this converter is termed a synchronous boost converter [8, 9, 10, 11].

In the present study, a boost converter was engineered and subjected to simulation to augment a 12-volt power source—specifically, the battery of an E-Scooter outfitted with a 24-volt, 600-watt BLDC motor—to a 24-volt load voltage. Subsequently, the efficiency and losses of the system designed with the conventional boost converter were compared with those of the system designed with the synchronous boost converter.

## 2. Materials and Methods

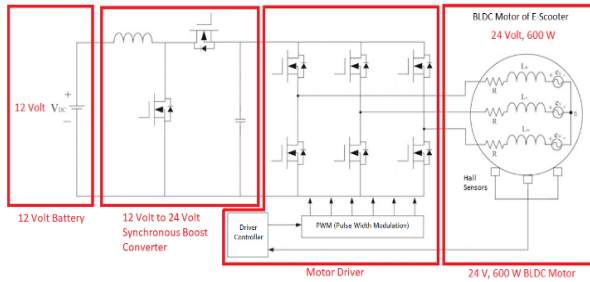


Fig. 1. Suggested E-Scooter Circuit Diagram

Electric scooters, colloquially known as E-Scooters, have gained significant traction in contemporary society due to their enhanced mobility and superior energy efficiency. The design paradigms for these scooters encompass a range of criteria, such as velocity, torque, energy efficiency, and functional requirements, which subsequently inform the selection of batteries, motors, and drive systems. Brushless Direct Current (BLDC) motors emerge as one of the predominant motor types deployed in these vehicular platforms. Figure-1 provides a schematic representation of the E-Scooter configuration explored in this manuscript.

As evident in the circuit schematic, a 12-volt battery is chosen as the power source. The BLDC motor, operating under nominal parameters of 24 volts and 600 watts, fulfills the energy requisites of the E-Scooter in a commendable manner. Due to the preordained operating voltage of 24 volts for the motor, there exists an inherent imperative to elevate the 12-volt battery voltage. In adherence to this objective, a Synchronous Boost Converter is employed, subsequently powering the driver circuitry of the BLDC motor.

The 12-volt batteries used in this E-Scooter circuit are among the most commonly available and easily accessible batteries in the market. Another reason for selecting a 12-volt battery is the convenience of using accessories in the E-Scooter that operate at this voltage. Connecting two batteries in series to obtain a 24-volt battery for this application would be heavy, bulky, and costly. Therefore, the 12-volt input voltage is boosted using a converter to obtain the voltage required by the motor.

The Synchronous Boost Converter effectively amplifies the 12-volt input voltage provided by the power source to a 24-volt output voltage. Additionally, through the controller, it balances the voltage drops on the battery side, increases the conversion ratio, and converts voltages below 12 volts to a stable 24 volts. With the converter, the impedance seen by the motor is increased, thereby enhancing the short-circuit withstand capability of the circuit. This results in drawing less current during fault conditions, ensuring the circuit's safety. Furthermore, better voltage regulation is achieved, resulting in a lower ripple ratio of the voltage waveform. Additionally, the supplied voltage to the motor driver can be increased during demand situations, enhancing the motor's overload capacity.

In addition to these benefits, the current level at the output of the Synchronous Boost Converter is twice that of the battery's output current. Consequently, motor and driver efficiencies increase. Transmission losses ( $I^2R$ ) decrease proportionally with the square of the current, allowing the use of thinner wires, reducing installation costs. The use of thinner wires also leads to lower voltage drops and losses. Therefore, the system's

efficiency clearly improves. Hence, the Synchronous Boost Converter is preferred.

### 2.1. Determination of Circuit Parameters of the Synchronous Boost Converter

For the Synchronous Boost Converter to be designed for the E-Scooter, there exist four parameters. These are the transmission ratio  $D$ , which provides the voltage ratio, the switching frequency  $T_s$  of the switches, the inductance value  $L$ , and the capacitance value  $C$ .

In this circuit, when the input voltage is 12 volts and the desired output voltage is 24 volts, according to Equation-1 [12], the value of  $D$  is calculated as 0.5. The switching frequency,  $T_s$ , will be selected as 50 kHz..

$$v = v_s D \quad (1)$$

When the current ripple is selected to be a maximum of 30 percent, the inductance value  $L$  is determined as 200  $\mu$  Henry according to Equation-2 [12].

$$2\Delta i_L = \frac{v_s}{L} DT_s \quad (2)$$

When the maximum voltage ripple is selected to be 12.5 percent, the capacitance value  $C$  is calculated as 470  $\mu$  Farads according to Equation-3 [12].

$$2\Delta v = \frac{v}{RC} DT_s \quad (3)$$

To ensure that the voltage values in this simulation are not strictly constant at 12 V/24 V, a controller has been designed. With this controller, in the event of a change in the input voltage, the desired voltage value will still be provided. Additionally, the reference value, which is the desired voltage value, can be adjusted.

The preferred controller in this case is the PI (Proportional-Integral) controller, and the values of  $K_p$  and  $K_i$  for the PI controller were determined using the Bode Diagram Method through the MATLAB software.

According to the analyses conducted by Mohan (2002), the Transfer Function of the Boost Converter was found as presented in Equation-4. Since the Transfer Function of the Synchronous Boost Converter can also be expressed using this function, it was utilized in determining the values of  $K_p$  and  $K_i$  [12].

$$G_{vd}(s) = \frac{V}{D} \frac{\left\{1 - \frac{sL}{D^2 R}\right\}}{\left\{1 + \frac{sL}{D^2 R} + \frac{s^2 LC}{D^2}\right\}} \quad (4)$$

This transfer function and input parameters have been defined in the MATLAB software as illustrated in Figure-2. Subsequently, the "sistool" command has been used to invoke the Bode plot screen.

```

1 - clear all;
2
3 - s = tf('s')
4
5 % r l c v d
6 - l = 0.0003;
7 - v = 12;
8 - c = 0.012;
9 - r = 1;
10 - d = 0.5;
11
12 - g = (v/d)*(1-s*(1/(d^2*r)))/((1+s*(1/(d^2*r))+s^2*1*c/(d^2)))
13
14 - sisotool(g)

```

**Fig. 2.** MATLAB Sistol Command

Following this command, the Bode Editor screen appears as shown in Figure-3. From this interface, the Step Response has been configured as desired. The Step Response should exhibit a stable graphical representation; for this purpose, one integrator and one zero have been added to the Root Locus Editor.

Subsequently, the gain value was selected to smooth the Step Response graph. When the Step Response is not stable, the designed controller system can lead to infinity or zero. Therefore, these operations become crucial.

From here, the values of Kp and Ki were determined as shown in Figure-4, and these obtained Kp, Ki values were entered into the simulation.

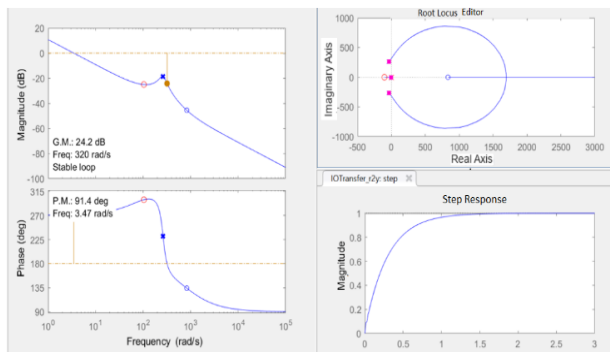


**Fig. 3.** Bode Editor

In Figure-4, the values were determined as Kp=0.0014929 and Ki=0.15242509 (102.1×0.0014929).

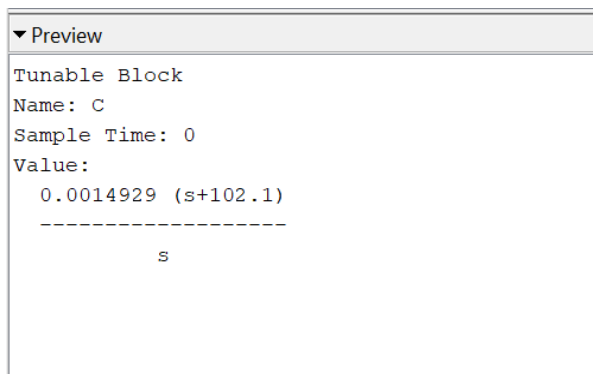


**Fig. 4.** Kp and Ki Values

## 2.2. Simulation of the Synchronous Boost Converter

In this section, the simulation of the Synchronous Boost Converter, with some of the circuit parameters obtained in Section 2.1., has been conducted. For the simulation, version 5.6 of PLECS software by Plexim was utilized.

The simulation of the Synchronous Boost Converter, utilizing certain circuit parameters from Section 2.1., is presented in Figure-5.

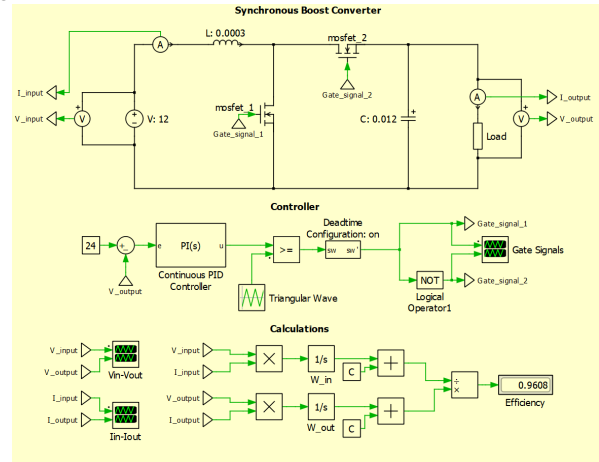


**Fig. 5.** PLECS Simulation of Synchronous Boost Converter

The parameters used in the circuit simulation presented in Table-1 are provided below.

**Table 1.** Synchronous Boost Converter Simulation Parameters

Parameter	Value	Unit
Input Voltage	12	Volt
Inductance	0.3 m	Henry
Capacitor	12 m	Farad
Resistance of Mosfet	0.011	Ohm
Mosfet Dead-time	0.5 μ	Second
PI Kp	0.0014929	-
PI Ki	0.15242509	-

The waveforms of the Synchronous Boost Converter simulation, as illustrated in Figure-5, are as follows.

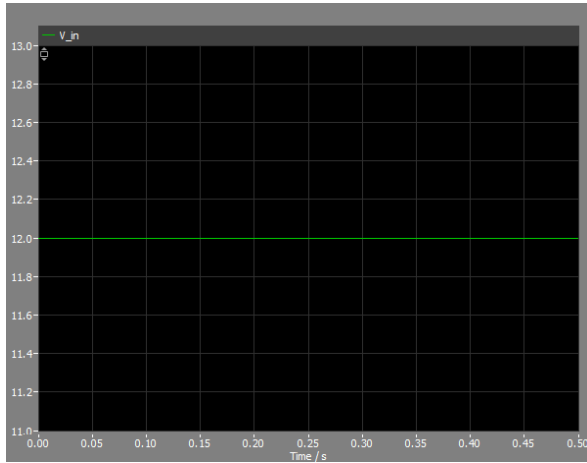


Fig. 6. Input Voltage

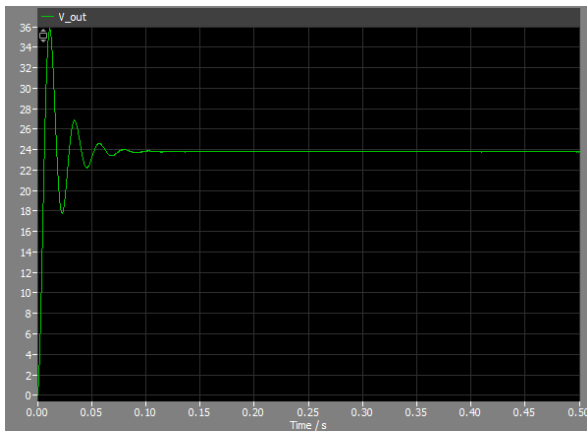


Fig. 7. Output Voltage

Input voltage and output voltage graphs were obtained using PLECS, as shown in Figure-6 and Figure-7. An input voltage value of 12 volts was provided, and given the transmission ratio of 0.5, the output voltage is expected to be 24 volts, as depicted in the graph.

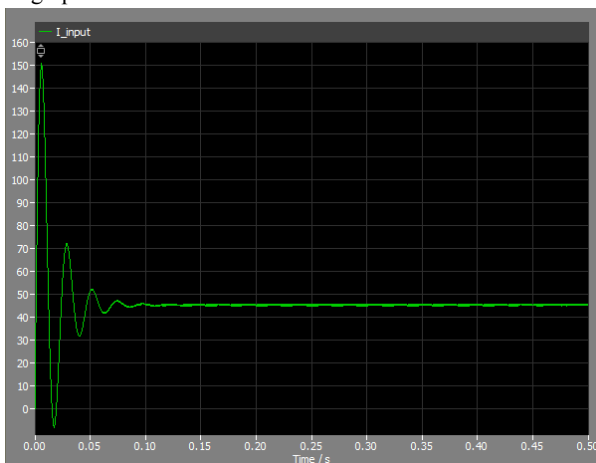


Fig. 8. Input Current

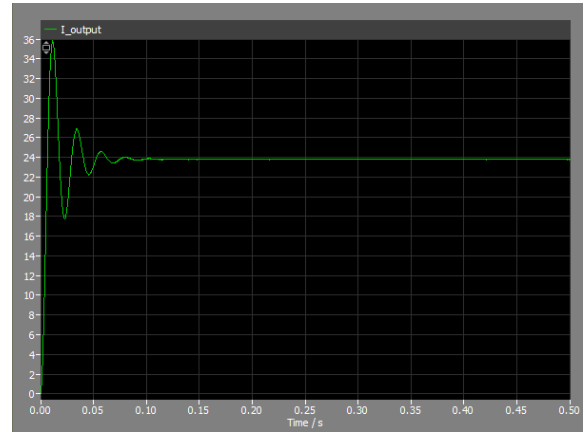


Fig. 9. Output Current

Figure-8 and Figure-9 depict the graphs of input current and output current. Also, as observed in the circuit, the inductor current is equal to the input current, and the capacitor voltage is equal to the output voltage.

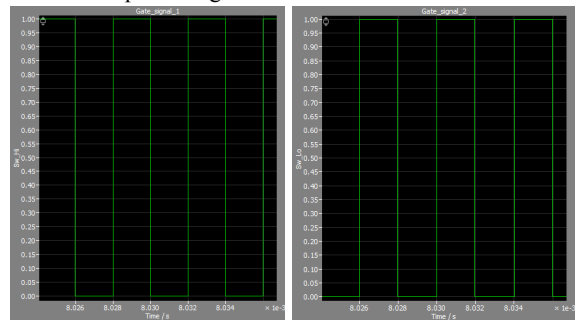


Fig. 10. Gate Signals

Figure-10 shows the gate signals of the Mosfets. As can be seen from these graphs, these Mosfets work reversibly to each other, that is, when one is in conduction, the other is in a cut-off state. In addition, due to the turn-on and turn-off times of the Mosfets, dead times are placed on these gate signals for the circuit to work properly and these short dead time ranges are shown in the graphs. Since the switching frequency is 50k Hz, the period of these switching signals is  $1/50k = 0.02$  ms as seen in the graphs.

As seen in Figure-5, the efficiency is 96.08%. The mathematical calculation with blocks here comes from the following formula, Equation-5:

$$\eta = \frac{Power_{output}}{Power_{input}} = \frac{Voltage_{output} \times Current_{output}}{Voltage_{input} \times Current_{input}} \quad (5)$$

The things that cause efficiency loss here are the power losses in the Mosfet. These losses are classified as conduction losses and switching losses. Switching losses are negligible compared to conduction losses. The conduction losses in the 2 mosfets are calculated as in Equation-6:

$$2 \times P_{on} = 2 \times D \times I_{on}^2 \times R_{ds} \quad (6)$$

$$2 \times 0.5 \times 24^2 \times 0.011 = 6.336 \text{ W} \quad (6)$$

### 2.3. Comparison of Synchronous Boost Converters and Conventional Boost Converters

In this section, using the PLECS software, a design similar to the Synchronous Boost Converter simulated in Figure-5 was created for a Conventional Boost Converter with the same input values. The design of this Conventional Boost Converter is illustrated in Figure-11.

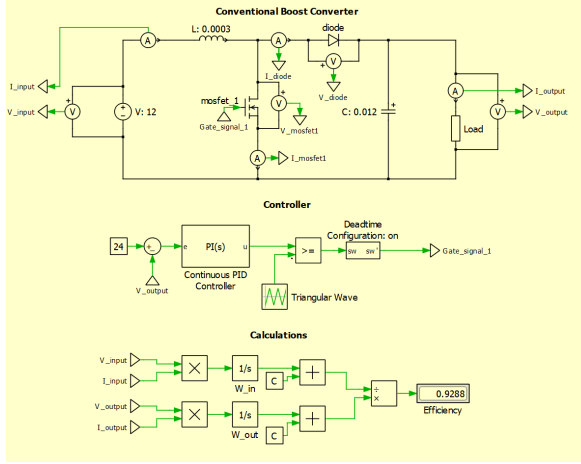


**Fig. 11.** PLECS Simulation of Conventional Boost Converter

As in Equation 6, the conduction losses of the diode and Mosfets are calculated as follows:

$$P_{on(mosfet)} = 0.5 \times 24^2 \times 0.011 = 3.168 \text{ W} \quad (7)$$

$$P_{on(diode)} = D \times I_{on} \times V_d = 0.5 \times 24 \times 1.5 = 18 \text{ W} \quad (8)$$

$$P_{on(total)} = P_{on(diode)} + P_{on(mosfet)} = 21.168 \text{ W} \quad (9)$$

As seen here, the conduction loss of the diode is almost 6 times the conduction loss of the mosfets and the total conduction losses in the conventional boost converter are 3.34 times the total conduction losses in the synchronous boost converter.

As seen in Figure-11, the efficiency of the Conventional Boost Converter is 92.88%, resulting in a loss ratio of 7.12%. On the other hand, Figure-5 shows that the efficiency of the Synchronous Boost Converter is 96.08%, corresponding to a 3.92% loss ratio. Consequently, the Synchronous Boost Converter operates 3.2% more efficiently than the Conventional Boost Converter. Moreover, the loss ratio has decreased from 7.12% to 3.92%, representing a 45% reduction in losses. This reduction is attributed to the power losses incurred by the Conventional Boost Converter due to the use of diodes and the voltage drop across these diodes, as discussed earlier.

### 3. Conclusions

In conclusion, the synchronous boost converter design implemented to enhance the efficiency of energy conversion systems used in E-Scooter applications has presented significant advantages when compared to the conventional boost converter. The process of raising the 12-volt battery output to 24 volts in a controllable manner has improved the system performance from various perspectives.

The advantages achieved through the developed synchronous boost converter include ensuring a controlled input voltage for

increased system stability, raising the impedance observed on the motor side to enhance short-circuit withstand capability, improving DC voltage regulation, and increasing the motor's overload capacity by exceeding 24 volts during peak demands.

Comparative analyses indicate that the losses of the synchronous boost converter have decreased by 45% compared to the conventional boost converter, resulting in an efficiency of 96.08%. This not only enhances the efficiency of the energy conversion process but also demonstrates the potential for providing more reliable and efficient energy management in E-Scooter applications.

### 7. References

- [1] Coruh, N., Urgun, S., Erfidan, T., & Ozturk, S. (2011). A simple and efficient implementation of interleaved boost converter. In Proceedings of the 2011 6th IEEE Conference on Industrial Electronics and Applications, ICIEA 2011 (pp. 2364–2368). <https://doi.org/10.1109/ICIEA.2011.5975988>
- [2] Küçük, T. V., Özbay, H., Candaş, Y., Karabacak, M., & Kale, M. (2016). Yüksek Frekans DA/DA Senkron Yükselten Dönüştürücü Tasarımı, Düzce Üniversitesi Bilim ve Teknoloji Dergisi.
- [3] Park, J. D., & Ren, Z. (2012). High efficiency energy harvesting from microbial fuel cells using a synchronous boost converter. Journal of Power Sources, 208, 322–327. <https://doi.org/10.1016/j.jpowsour.2012.02.035>.
- [4] Dittmer, G. (2015). Buck or boost: rugged, fast 60V synchronous controller does both. In Analog Circuit Design (pp. 325–326). Elsevier, <https://doi.org/10.1016/b978-0-12-800001-4.00155->.
- [5] Meng He. (2016). Synchronous or Nonsynchronous Topology? Boost System Performance with the Right DC-DC Converter. Maxim Integrated, 1–4. Retrieved from <https://www.maximintegrated.com/en/design/technical-documents/app-notes/6/6129.html>
- [6] Hinov, N., Arnaudov, D., Valchev, V., & Vuchev, S. (2017). Comparative loss analysis of boost and synchronous boost DC-DC converters. In 2017 26th International Scientific Conference Electronics, ET 2017 - Proceedings (Vol. 2017-January, pp. 1–4). Institute of Electrical and Electronics Engineers Inc. <https://doi.org/10.1109/ET.2017.8124347>
- [7] Mahmoud, S. M., El-Sherif, M. Z., Abdel-Aliem, E. S., & Nashed, M. N. F. (2013). Studying Different Types of Power Converters Fed Switched Reluctance Motor. International Journal of Electronics and Electrical Engineering, 281–290. <https://doi.org/10.12720/ijeec.1.4.281-290>
- [8] Pradhan, A., & Panda, B. (2018). A simplified design and modeling of boost converter for photovoltaic system. International Journal of Electrical and Computer Engineering, 8(1), 141–149. <https://doi.org/10.11591/ijeec.v8i1.pp141-149>
- [9] Nowakowski, R., & Nin. (2009). Efficiency of synchronous versus nonsynchronous buck converters. Analog Applications Journal Texas Instruments Incorporated 4Q, 15–18.
- [10] Yılmaz, M., Çorapsız, M. F., & Çorapsız, M., R. (2020). Voltage Control of Cuk Converter with PI and Fuzzy Logic Controller in Continuous Current Mode. Balkan Journal of Electrical & Computer Engineering, Vol 8.
- [11] Pistoia, G. (2009). Battery operated devices and systems: From portable electronics to industrial products. Chapter 2: Battery Categories and Types, 40.
- [12] Mohan, N. (2003). Power Electronics Converters, Applications and Design 3rd. John Wiley & Sons.